

Thermoanalytical studies of natural potassium, sodium and ammonium alunites

János Kristóf · Ray L. Frost · Sara J. Palmer ·
Erzsébet Horváth · Emma Jakab

Received: 25 May 2009 / Accepted: 21 October 2009 / Published online: 28 November 2009
© Akadémiai Kiadó, Budapest, Hungary 2009

Abstract Dynamic and controlled rate thermal analysis (CRTA) has been used to characterise alunites of formula $[M(Al)_3(SO_4)_2(OH)_6]$ where M^+ is the cations K^+ , Na^+ or NH_4^+ . Thermal decomposition occurs in a series of steps: (a) dehydration, (b) well-defined dehydroxylation and (c) desulphation. CRTA offers a better resolution and a more detailed interpretation of water formation processes via approaching equilibrium conditions of decomposition through the elimination of the slow transfer of heat to the sample as a controlling parameter on the process of decomposition. Constant-rate decomposition processes of water formation reveal the subtle nature of dehydration and dehydroxylation.

Keywords Alunite thermal analysis · Controlled rate thermal analysis · Dehydration · Dehydroxylation

Introduction

Interest in alunites stems from a number of reasons: (a) firstly there is the possible discovery of alunites on Mars and possibly other planets [1, 2]. Such findings imply the presence of water either at present or at some time in the planetary past, since alunites are only formed from solution through precipitation and crystallisation processes. Interest in such minerals and their thermal stability rests with the possible identification of these minerals and dehydrated paragenetically related minerals. There have been many studies on related minerals such as the Fe(II) and Fe(III) sulphate minerals and jarosites [3–7]. (b) The importance of alunite formation and its decomposition depends upon its presence in soils, sediments and evaporite deposits [8–10]. These types of deposits have formed in acid soils where the pH is less than 3.0 pH units. Such acidification results from the oxidation of pyrite which may be from bacterial action or through air-oxidation. (c) Thirdly alunites are important from an environmental point of view. Alunites are minerals which can function as collectors of heavy metals and low concentrations can be found in the natural alunites. Such minerals can act as a significant environmental sink.

One of the difficulties associated with the analysis of alunites is that they are often poorly crystalline, making detection using XRD techniques difficult. Another problem associated with the study of alunites is their thermodynamic stability. Often the minerals are formed from acid-sulphate rich environments such as acid mine drainage and acid-sulphate soils and as such their solubility is controlled by climatic conditions, in particular the temperature. Such minerals lend themselves for thermal analysis. Interestingly, there have been few recent studies on the thermal analysis of alunites. The reason for this is unclear. Perhaps

J. Kristóf
Department of Analytical Chemistry, University of Pannonia,
PO Box 158, 8201 Veszprém, Hungary

R. L. Frost (✉) · S. J. Palmer
Inorganic Materials Research Program, School of Physical and
Chemical Sciences, Queensland University of Technology, 2
George Street, GPO Box 2434, Brisbane, QLD 4001, Australia
e-mail: r.frost@qut.edu.au

E. Horváth
Institute of Environmental Engineering, University of Pannonia,
PO Box 158, 8201 Veszprém, Hungary

E. Jakab
Central Research Institute for Chemistry, Hungarian Academy of
Science, PO Box 17, 1525 Budapest, Hungary

it is because of the variation in composition which occurs with natural minerals. Such variation can be overcome with the use of synthetic minerals. The first recorded thermal analysis of alunite occurred in 1919. Early studies focussed on the effect of alunite impurity on the thermal treatment of other chemicals. Many studies occurred when new equipment became available. Recently thermal analysis has been used to enhance the understanding of the stability of minerals [11–23].

In this work, as part of our studies of secondary mineral formation and their stability, we report the comparison of the thermal analysis of selected natural alunites using both dynamic and controlled rate thermal analysis techniques.

Experimental

Minerals

The alunites were obtained from the Mineralogical Research Company, Australia. The minerals were phase analysed by powder X-ray diffraction and were analysed for chemical composition by EDX methodology.

Thermal analysis

Conventional thermal analysis experiment

Thermal decomposition of the alunites was carried out in a Derivatograph PC type thermoanalytical equipment (Hungarian Optical Works, Budapest, Hungary) capable of recording the thermogravimetric (TG), derivative thermogravimetric (DTG) and differential thermal analysis (DTA) curves simultaneously. The samples were heated in a ceramic crucible in static air atmosphere at a rate of $5\text{ }^{\circ}\text{C min}^{-1}$. The thermoanalytical equipment is coupled to a mass spectrometer. In order to understand the gas evolution pattern, mass spectrometric identification of gaseous decomposition products has been carried out in argon atmosphere in a Perkin Elmer TGS-2 type thermobalance connected to a Hayden HAL 2/301 PIC type mass spectrometer. The heating rate was $10\text{ }^{\circ}\text{C min}^{-1}$. As water produces m/z 17 fragment ion, the contribution of water was subtracted from the intensity curve of m/z 17. Thus, the m/z 17 ion represent only NH_3^+ molecular ion.

Controlled rate thermal analysis experiment

Thermal decomposition of the alunite samples under CRTA conditions was carried out in the Derivatograph under static air in an open ceramic crucible at a pre-set, constant decomposition rate of 0.1 mg min^{-1} . (Below this threshold value the samples were heated under dynamic

conditions at a uniform rate of $1.0\text{ }^{\circ}\text{C min}^{-1}$). With the quasi-isothermal, quasi-isobaric heating program of the instrument the furnace temperature was regulated precisely to provide a uniform rate of decomposition in the main decomposition stage.

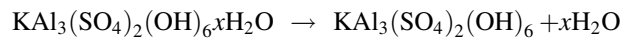
Results and discussion

The dynamic TG, DTG and DTA patterns of potassium, sodium and ammonium alunites are shown in Figs. 1, 2 and 3 respectively. The results of the conventional constant rate heating experiment are reported in Table 1. The controlled rate thermal analysis results are reported in Table 2 and the CRTA patterns of potassium, sodium and ammonium alunites are shown in Figs. 5, 6 and 7.

Dynamic thermal analysis of potassium alunite

The behaviour of the thermal decomposition is different for the potassium, sodium and ammonium alunites. The thermal decomposition of potassium alunites takes place in four mass loss steps as shown in Fig. 1. The mass loss values belonging to the individual decomposition steps are summarised in Table 1. DTG peak maxima are observed at 246, 513, 797 and 908 $^{\circ}\text{C}$. The DTA patterns shows minima at 246, 517 and 795 $^{\circ}\text{C}$ indicating endothermic steps in the thermal decomposition process.

Step 1: dehydration The loss of crystallization water takes place at 246 $^{\circ}\text{C}$ according to the following equation:



Based on the TG curve, the exact amount of crystallization water was 1.31 moles.

Step 2: dehydroxylation Dehydroxylation occurs at 513 $^{\circ}\text{C}$ resulting in the evolution of 3 moles of water:

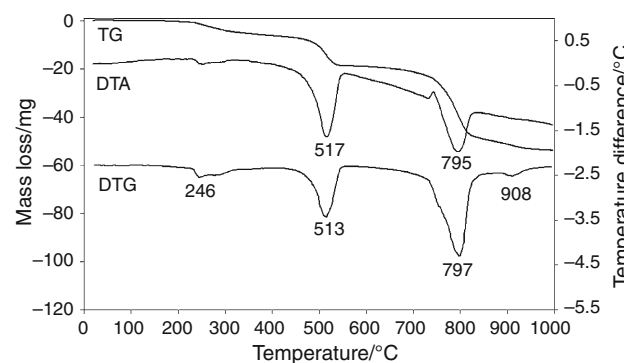


Fig. 1 TG–DTG–DTA curves of potassium alunite under dynamic heating

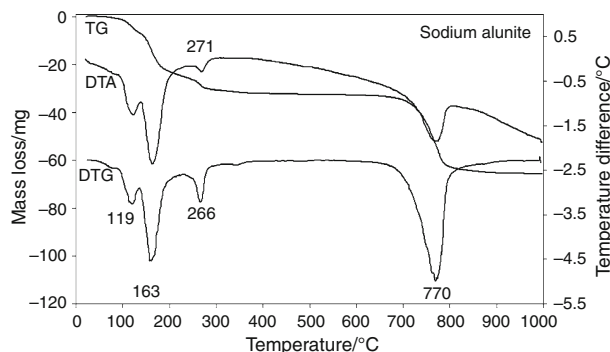


Fig. 2 TG–DTG–DTA curves of sodium alunite under dynamic heating

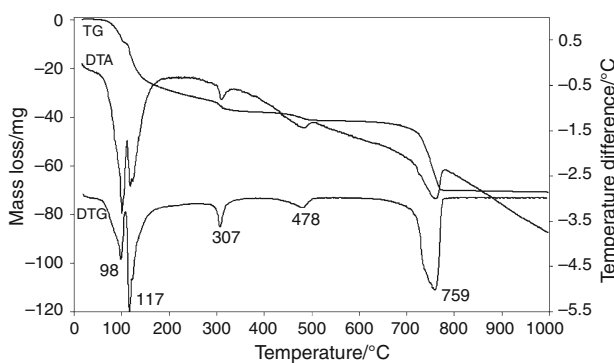
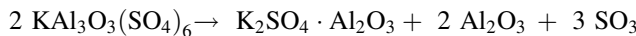


Fig. 3 TG–DTG–DTA curves of ammonium alunite under dynamic heating



(the theoretical mass loss is 13.0%, the observed loss is 11.6%).

Step 3: desulphation The desulphation reaction occurs in two steps at 797 and 908 °C leading to the formation of $\text{K}_2\text{SO}_4 \cdot \text{Al}_2\text{O}_3$ and alumina as follows:



(the theoretical mass loss in this reaction is 33.34%, the actual loss is 36.37%).

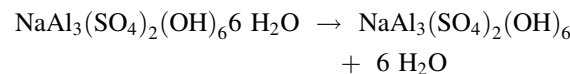
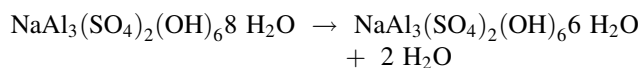
Table 1 Temperature and mass loss data of the decomposition of alunite samples under dynamic conditions

Sample: NH ₄ alunite			Sample: K alunite			Sample: Na alunite		
Temperature range/°C	Mass loss (sample mass: 86.18/mg)		Temperature range/°C	Mass loss (sample mass: 115.04/mg)		Temperature range/°C	Mass loss (sample mass: 95.12/mg)	
	mg	%		mg	%		mg	%
32–106	9.3	10.8	115–399	6.2	5.4	35–135	6.8	7.1
106–259	22.9	26.6	399–563	12.6	11.0	135–227	18.2	19.1
259–388	6.0	7.0	563–851	30.5	26.5	227–403	7.3	7.7
388–529	3.5	4.1	851–992	4.5	3.9	403–973	33.4	35.1
577–791	28.6	33.2						

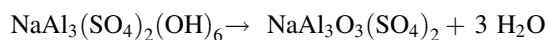
Dynamic thermal analysis of sodium alunite

The thermal decomposition behaviour of the sodium alunite appears significantly different to that of the potassium alunite (Fig. 2). The three mass loss steps that appear in the DTG curve at 119, 163 and 266 °C belong to the liberation of water, while desulphation occurs in a single process at 770 °C.

Step 1: dehydration Dehydration is believed to take place in two steps resulting in all together the release of 7.88 moles of water. Therefore, the following dehydration mechanism is proposed:



Step 2: dehydroxylation Dehydroxylation is believed to take place at 266 °C as follows:



(the theoretical mass loss in this process is 9.54%, while the actual one is 10.41%).

Step 3: desulphation Sulphur trioxide is released at 770 °C in accordance with the following equation based on stoichiometric calculations:



(the theoretical mass loss in this reaction is 46.54%, while the actual amount of SO₃ released is 53.17%).

Dynamic thermal analysis of ammonium alunite

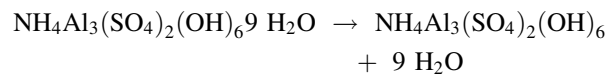
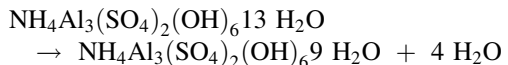
The thermal decomposition of ammonium alunite shows peaks in the DTG curve at 98, 117, 307, 478 and 759 °C (Fig. 3). Endothermic peaks in the DTA curves occur at similar positions. The TG-MS pattern (Fig. 4) is essential to reveal the complicated nature of decomposition. In the

Table 2 Temperature and mass loss data of the decomposition of alunite samples under CRTA conditions

Sample: NH ₄ alunite			Sample: K alunite			Sample: Na alunite		
Temperature range/°C	Mass loss (sample mass: 139.12/mg)		Temperature range/°C	Mass loss (sample mass: 168.11/mg)		Temperature range/°C	Mass loss (sample mass: 158.38/mg)	
	mg	%		mg	%		mg	%
33–66	17.9	12.9	118–245	4.1	2.4	24–91	5.6	3.5
66–90	14.7	10.6	245–302	3.3	2.0	91–112	8.3	5.2
90–235	22.5	16.2	302–379	2.2	1.3	112–167	24.9	15.7
235–368	7.1	5.1	379–520	18.1	10.8	167–234	10.6	6.7
368–506	6.1	4.4	520–597	1.1	0.7	234–296	3.3	2.1
						296–412	2.3	1.5
						412–569	0.8	0.5

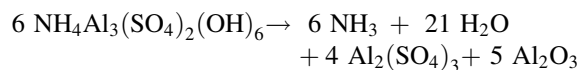
first step water is released, while the two decomposition steps between 300 and 550 °C belong to the simultaneous evolution of water and ammonia. In the last step of decomposition sulphur trioxide is liberated, only. However, sulphur trioxide is not stable under mass spectrometric conditions; therefore, the evolution of sulphur dioxide and oxygen can be monitored.

Step 1: dehydration Since water elimination in the first two steps (at 98 and 117 °C) belongs to dehydration, the total amount of crystallization water is 13.0 moles. Thus, the following dehydration mechanism is proposed:



Step 2: dehydroxylation and de-ammonification At 307 and 478 °C dehydroxylation water and ammonia are

liberated simultaneously. With faster heating the two processes merge together as it is witnessed in Fig. 4. Thus, the proposed mechanism of decomposition is as follows:



(the theoretical mass loss in this process is 20.37%, while the actual loss is 17.60%).

Step 3: desulphation The decomposition step of the mineral observed at 759 °C is interpreted by liberation of sulphur trioxide as follows:



The controlled rate thermal analysis experiment

The thermal decomposition patterns of the potassium, sodium and ammonium alunite samples recorded under CRTA decompositions are shown in Figs. 5, 6 and 7. The mass loss data are summarised in Table 2. The dehydration process of potassium alunite (Fig. 5) under the slow heating rate of 1 °C min⁻¹ can be resolved to four overlapping steps between 100 and 200 °C, at 222, 257 and 326 °C. During the

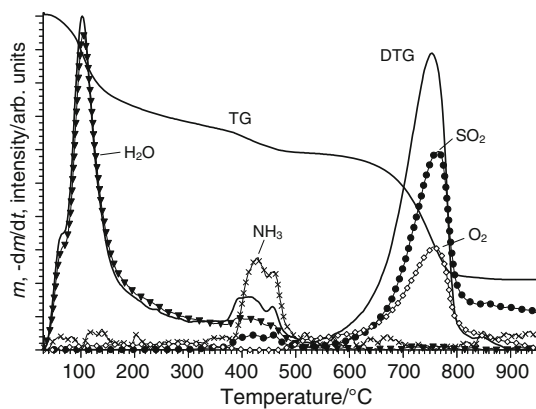


Fig. 4 Thermogravimetric and mass spectrometric ion intensity curves of ammonium alunite (m/z 17: NH_3^+ , m/z 18: H_2O^+ , m/z 32: O_2^+ , m/z 64: SO_2^+)

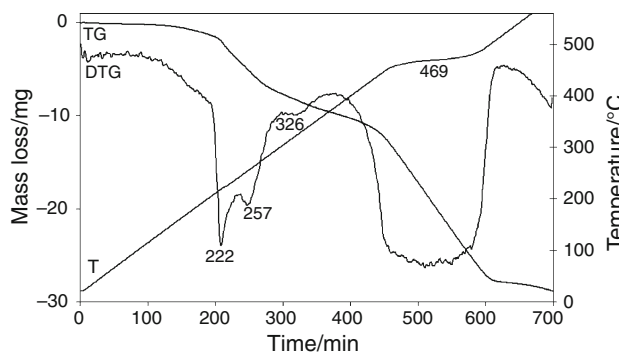


Fig. 5 Thermal decomposition pattern of potassium alunite under CRTA conditions

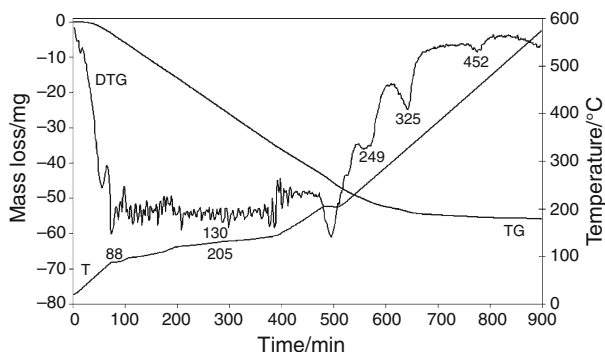


Fig. 6 Thermal decomposition pattern of sodium alunite under CTRA conditions

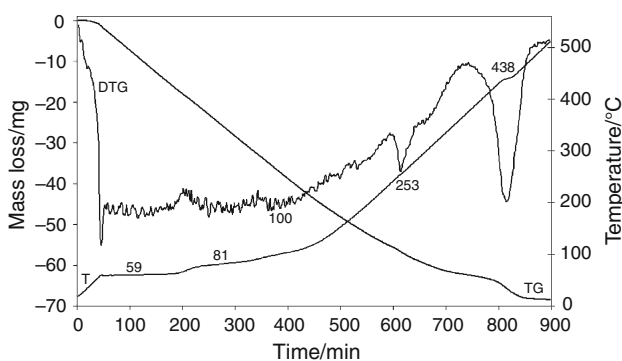


Fig. 7 Thermal decomposition pattern of ammonium alunite under CTRA conditions

dynamic experiment only two dehydration steps could be identified in the DTG curve. The controlling rate of 0.1 mg min^{-1} was not reached until 400°C . Dehydroxylation took place in a homogeneous process represented by an isothermal, constant rate of water evolution at 469°C .

Dehydration of sodium alunite (Fig. 6) under CTRA conditions took place in two steps (similarly, to the dynamic experiment) up to 200 min and between 200 and 400 min . The controlling level of 0.1 mg min^{-1} was reached in both steps resulting in a quasi-isothermal pattern of water evolution at 88 and 130°C . Above 400 min dehydroxylation took place in four steps at 200 , 249 , 325 and 452°C under the slow heating (the rate of decomposition did not reach the controlling level of 0.1 mg min^{-1}). This experiment revealed the subtle nature of dehydroxylation which was not observed in the dynamic experiment.

The dehydration of the ammonium alunite sample (Fig. 7) took place up to 600 min in three isothermal steps at 59 , 81 and 100°C . In the dynamic experiment only two steps can be distinguished. The parallel process of dehydroxylation and de-ammonification takes place in two steps (similarly, to the dynamic experiment) under the controlling level of 0.1 mg min^{-1} .

Conclusions

Natural aluminates show characteristic thermogravimetric patterns with thermal decomposition steps: (a) dehydration, (b) well-defined dehydroxylation and (c) desulphation. While the patterns of dehydration and dehydroxylation (as well as the amounts of crystallisation water) differ significantly depending on the nature of the cation, desulphation is a rather homogeneous process (the DTG peak temperatures fall in the range between 760 and 800°C for all the three samples).

CRTA offers a better resolution and a more detailed interpretation of the decomposition processes via approaching equilibrium conditions of decomposition through the elimination of the slow transfer of heat to the sample as a controlling parameter on the process of decomposition. With this technique differences in the dehydration and decomposition patterns can be revealed suspecting a more complex pattern of decomposition as revealed under dynamic heating.

It is very important to be able to thermally characterise minerals such as aluminates which may be found on planets such as Mars. The existence of aluminates on Mars would confirm the presence of water at some time in the past as such minerals are only formed from solution. The thermal stability of aluminates is most important as there is a need to find the temperature range over which the minerals are stable, since wide temperature ranges are likely on planets.

Acknowledgements This research was supported by the Hungarian Scientific Research Fund (OTKA) under Grant No. K62175. The financial and infra-structure support of the Queensland University of Technology Inorganic Materials Research Program is gratefully acknowledged.

References

1. Serna CJ, Parada Cortina C, Garcia Ramos JV. Infrared and Raman study of alunite-jarosite compounds. *Spectrochim Acta*. 1986;42A:729–34.
2. Tsutsumi S, Otsuka R. Thermal studies of the alunite-natrolalunite series, $(K,\text{Na})\text{Al}_3(\text{SO}_4)_2(\text{OH})_6$. In: Proceedings of the 5th international conference on thermal analysis; 1977. p. 456–457.
3. Alias Perez LJ, Girella F. Differential thermal analysis of jarosite-alunite solid solutions and mixtures. *Estudios Geologicos* (Madrid). 1968;24:79–83.
4. Atencio D, Hypolito R. $\text{Fe}_2\text{O}_3\text{-SO}_3\text{-H}_2\text{O}$ system: mineralogical aspects. *Anais da Associacao Brasileira de Quimica*. 1993;41–42:32–8.
5. Bishop JL, Murad E. The visible and infrared spectral properties of jarosite and alunite. *Am Mineral*. 2005;90:1100–7.
6. Cocco G. Differential thermal analysis of some sulfate minerals. *Period Miner*. 1952;21:103–38.
7. Frost RL, Wain D, Martens WN, Locke AC, Martinez-Frias J, Rull F. Thermal decomposition and X-ray diffraction of sulphate efflorescent minerals from El Jaroso Ravine, Sierra Almagrera, Spain. *Thermochim Acta*. 2007;460:9–14.

8. Frost RL, Weier ML, Kloprogge JT, Rull F, Martinez-Frias J. Raman spectroscopy of halotrichite from Jaroso, Spain. *Spectrochim Acta*. 2005;62:176–80.
9. Frost RL, Weier ML, Martens W. Thermal decomposition of jarosites of potassium, sodium and lead. *J Therm Anal Calorim*. 2005;82:115–8.
10. Frost RL, Wills RA, Martens W, Weier W, Reddy BJ. NIR spectroscopy of selected iron(II) and iron(III) sulphates. *Spectrochim Acta*. 2005;62A:42–60.
11. Frost RL, Hales MC, Martens WN. Thermogravimetric analysis of selected group (II) carbonate minerals—implication for the geosequestration of greenhouse gases. *J Therm Anal Calorim*. 2009;95:999–1005.
12. Palmer SJ, Spratt HJ, Frost RL. Thermal decomposition of hydrotalcites with variable cationic ratios. *J Therm Anal Calorim*. 2009;95:123–9.
13. Carmody O, Frost R, Xi Y, Kokot S. Selected adsorbent materials for oil-spill cleanup. A thermoanalytical study. *J Therm Anal Calorim*. 2008;91:809–16.
14. Frost RL, Locke A, Martens WN. Thermogravimetric analysis of wheatleyite $\text{Na}_2\text{Cu}^{2+}(\text{C}_2\text{O}_4)_2 \cdot 2\text{H}_2\text{O}$. *J Therm Anal Calorim*. 2008;93:993–7.
15. Frost RL, Locke AJ, Hales MC, Martens WN. Thermal stability of synthetic aurichalcite. Implications for making mixed metal oxides for use as catalysts. *J Therm Anal Calorim*. 2008;94:203–8.
16. Frost RL, Locke AJ, Martens W. Thermal analysis of beaverite in comparison with plumbojarosite. *J Therm Anal Calorim*. 2008;92:887–92.
17. Frost RL, Wain D. A thermogravimetric and infrared emission spectroscopic study of alunite. *J Therm Anal Calorim*. 2008;91:267–74.
18. Hales MC, Frost RL. Thermal analysis of smithsonite and hydrozincite. *J Therm Anal Calorim*. 2008;91:855–60.
19. Palmer SJ, Frost RL, Nguyen T. Thermal decomposition of hydrotalcite with molybdate and vanadate anions in the interlayer. *J Therm Anal Calorim*. 2008;92:879–86.
20. Vagvolgyi V, Daniel LM, Pinto C, Kristof J, Frost RL, Horvath E. Dynamic and controlled rate thermal analysis of attapulgite. *J Therm Anal Calorim*. 2008;92:589–94.
21. Vagvolgyi V, Frost RL, Hales M, Locke A, Kristof J, Horvath E. Controlled rate thermal analysis of hydromagnesite. *J Therm Anal Calorim*. 2008;92:893–7.
22. Vagvolgyi V, Hales M, Martens W, Kristof J, Horvath E, Frost RL. Dynamic and controlled rate thermal analysis of hydrozincite and smithsonite. *J Therm Anal Calorim*. 2008;92:911–6.
23. Zhao Y, Frost RL, Vagvolgyi V, Waclawik ER, Kristof J, Horvath E. XRD, TEM and thermal analysis of yttrium doped boehmite nanofibres and nanosheets. *J Therm Anal Calorim*. 2008;94:219–26.